

Erratum

(African Health Sciences 2013; 13(2): 243 – 251)

Differential expressed genes in ECV304 Endothelial-like Cells infected with Human Cytomegalovirus

Yali Zhang¹, Wenli Ma², Xiaoyang Mo³, Haiquan Zhao², Huanying Zheng⁴, Changwen Ke⁴, Wenling Zheng², *Yanyang Tu⁵, *Yongsheng Zhang⁵

1. Department of Clinical Laboratory Science, Guiyang Medical College, Guiyang, Guizhou 550004, China
2. Institute of Genetic Engineering, Southern Medical University, Guangzhou, Guangdong 510515, China
3. The Center for Heart Development, Key Lab of National Education Ministry, College of Life Sciences, Hunan Normal University, Changsha, Hunan, 410006 China
4. Guangdong Province Center of Disease Control Virology Section, Guangzhou, Guangdong 510033, China
5. Department of Experimental Surgery, Tangdu Hospital, The Forth Military Medical University, Xi'an, Shannxi, 710038, China

Abstract

Background: Human cytomegalovirus (HCMV) is a virus which has the potential to alter cellular gene expression through multiple mechanisms.

Objective: With the application of DNA microarrays, we could monitor the effects of pathogens on host-cell gene expression programmes in great depth and on a broad scale.

Methods: Changes in mRNA expression levels of human endothelial-like ECV304 cells following infection with human cytomegalovirus AD169 strain was analyzed by a microarray system comprising 21073 60-mer oligonucleotide probes which represent 18716 human genes or transcripts.

Results: The results from cDNA microarray showed that there were 559 differential expressed genes consisted of 471 up-regulated genes and 88 down-regulated genes. Real-time qPCR was performed to validate the expression of 6 selected genes (RPS24, MGC8721, SLC27A3, MST4, TRAF2 and LRRC28), and the results of which were consistent with those from the microarray. Among 237 biology processes, 39 biology processes were found to be related significantly to HCMV-infection. The signal transduction is the most significant biological process with the lowest p value ($p=0.005$) among all biological process which involved in response to HCMV infection.

Conclusion: Several of these gene products might play key roles in virus-induced pathogenesis. These findings may help to elucidate the pathogenic mechanisms of HCMV caused diseases.

Key words: Human cytomegalovirus, microarray, Gene expression profiling; infectomics

African Health Sciences 2013; 13(4): 864 - 879 <http://dx.doi.org/10.4314/ahs.v13i4.2>

Introduction

Human cytomegalovirus (HCMV), which is a species of the cytomegalovirus family of viruses and is alternatively known as human herpesvirus-5 (HHV-5), is the most common pathogen causing congenital infection and primary infection during pregnancy¹.

It can cause life-threatening systemic infections in immunocompromised patients and has been recognized as a risk factor for vascular diseases, like arterial restenosis and atherosclerosis². The impacts of HCMV has increased in recent decades due to the rising risk of organ allografting, immunosuppressive treatment, radiation damage, malignant tumor, and human immunodeficiency virus (HIV)-infected patients^{3,4}. As the number of patients suffering from HCMV infections has steadily increased, there is a growing need to understand the molecular mechanism by which the virus causes disease.

*Corresponding authors:

Yongsheng Zhang, Yanyang Tu
Tangdu Hospital
The Forth Military Medical University
Xi'an 710038, P.R China
E - mail : z h a n g y s _ t d @ 1 6 3 . c o m ,
tu.fmmu@gmail.com

HCMV can infect many different cell types *in vivo*, such as smooth muscle cells, endothelial cells, epithelial cells, neuronal cells, monocyte/macrophage lineage cells and so on⁵⁻⁷. Cytopathic effects of HCMV are varied in different tissues and cell lines. Endothelial cells are natural sites of HCMV infection *in vivo* following a primary infection and are a possible viral reservoir, suggesting that endothelial cells may play a role in viral spread and persistence^{8,9}. HCMV infection of endothelial cells is also associated with atherosclerosis and transplant vascular sclerosis in HCMV-infected patients, pointing to the possible role that infected endothelial cells may play in HCMV-mediated diseases. However, the specific mechanisms by which HCMV infects endothelial cells remain unclear. Virus-induced phenotypic changes in host cells are often accompanied with marked changes in gene expression that are related with the pathogenic mechanisms. In the last few years, studies showed changes in gene expression that occur on different host cell types with different types of viral infections¹⁰. Therefore, analysis of changes in gene expression that occur on infection of endothelial cells with HCMV will be better for revealing the pathogenic mechanisms of HCMV.

DNA expression profiling microarrays are designed to monitor of hundreds and thousands of mRNA levels, and therefore, analysis of those data from microarray experiment can provide us with important information to understand the biological processes and complex pathogenesis of infectious diseases. This technology has also been used in studies on different target cells infected with HCMV, which have different performance depending on probe characteristics, array density, sample labeling methods and the characteristics of target cell¹¹⁻¹⁴. Because most studies aimed at human foreskin fibroblast (HFF) as target cell which was infected by HCMV, gene expression profiling of endothelial cells infected HCMV has not yet been studied intensively.

In this study, we monitored the effects of HCMV on ECV304 gene expression profiling using 60-mer high-density oligo microarray, which allowed us to explore the effects of HCMV on endothelial cell gene expression programme in great depth and on a broad scale. Transcriptional-profiling study has also made us to further understand the mechanism of infectious disease process.

Methods

Cell Culture and Virus Infection

ECV304 cells were obtained from Southern Medical University, Guangzhou. The human cytomegalovirus (HCMV) AD169 strain was kindly provided by Medical College of China Central South University. ECV304 cells were cultured in maintenance medium (MEM, Gibco, US) supplemented with 10% fetal calf serum, glutamine, sodium bicarbonate, penicillin and streptomycin at 37°C with 5% CO₂ in a humidified incubator. The HCMV AD169 strain (4.0 logTCID₅₀/0.1ml) was prepared by harvesting the supernatant of infected cells 6 days post-infection (p.i.). The amount of infectious virus released from the infected cells was determined by the TCID₅₀ method. The ECV304 cells that had been confluent for at least 3 days in a Cell Culture Flasks (25cm²) were infected with 1mL purified HCMV virions, which was prepared by harvesting the supernatant of infected cells 6 days post-infection (4.0 logTCID₅₀ /0.1ml). Confluent cells were then grown in maintenance medium with only 2% fetal calf serum to avoid overstimulating cell growth prior to infection. One batch of uninfected ECV304 cells served as control, while other batches were infected with HCMV AD169 strain.

Detection of HCMV DNA in ECV304 cells by PCR

The early protein gene of HCMV genome was amplified by PCR using the primer set: (forward: 5'-CCA AGC GGC CTC TGA TAA CCA AG-3') and (reverse: 5'-CAG CAC CAT CCT CCT CTT CCT CT -3'), which could be used to produce a 430-bp fragment. PCR was performed in 50 µl reaction mixtures, containing 0.5µg of DNA template, 0.4 µM of each primer, 25 µl of 2×Premix and 18µl of ddH₂O. Cycling conditions consisted of an initial denaturation of 5 min at 94°C; 35 cycles, each cycle consisting of 1 min at 94°C, 30 s at 65°C, and 1 min at 72°C; followed by a final extension step at 72°C for 5 min. The PCR products were electrophoresed using 1.5% agarose gels (Shanghai Yito Enterprise, Shanghai, China) and detected by ethidium bromide staining.

Detection of HCMV pp65 protein expression by immunofluorescence

HCMV pp65 protein expression was demonstrated by immunofluorescence. ECV304 cells were grown on chamber slides and infected with HCMV for 4 days. Infected and uninfected cells were fixed with mixture of 2% paraformaldehyde and 0.1% Triton X-100 for 30 min at room temperature, washed twice with PBS, blocked with normal goat serum for 20

min, and then incubated with mouse anti-HCMV pp65 (US Biological, USA) for 30 min at 37°C. After rinsing with PBS for five times, slides were incubated with FITC-conjugated secondary antibody for 30 min at 37 °C. The slides were visualized with fluorescent microscopy (Nikon TE-2000, US).

Microarray hybridization and analysis

Total RNA from the infected and uninfected cells were extracted using Trizol reagent (Shenergy Biocolor BioScience & Techonology company, Shanghai) according to the manufacturer's instructions. The quality of total RNA for all microarray experiments was controlled by ultraviolet spectrophotometer DU530 (Beckman) and BioAnalyzer 2100 (Agilent, Palo Alto, CA, USA). Total RNAs (500 ng) from the uninfected and infected ECV304 cells were reversed-transcribed and labeled with Cy5- and Cy3-dCTP using Low Input RNA Fluorescent Linear Amplification Kit (Agilent, Palo Alto, CA, USA), respectively. The Cy5- and Cy3- labeled targets are purified using Rneasy mini spin columns (Qiagen), and then mixed and hybridized to the 60mer Human 1A Oligo Microarray Kit (Agilent, Palo Alto, CA, USA). The hybridization volume of 450µl consisted of 7µg of each Cy3- and Cy5-labeled sample, 50µl 10×control target and 225µl 2×hybridization buffer. The mixture was vibrated and centrifuged shortly, then pipetted on a new coverslip and covered with Agilent microarray. The slides were incubated at 60°C for 16 h in the hybridization chamber, and subsequently washed twice with the solution containing 6×SSC and 0.005% Triton X-102 for 10 min at room temperature, followed by ice-cold solution (0.1×SSC, 0.005% Triton X-102) for 5 min. The slides were then dried with nitrogen and stored in dark place. Scanning was performed with an Agilent 2565BA scanner (Agilent, Palo Alto, CA, USA), and the data of the images were acquired using Agilent G2567AA Feature Extraction Software (version 7.1.1). The features were automatically loaded with a grid file and calculated the centroid positions of each spot on the microarray. The Cookie Cutter method was used to define the features. Filtering was automatically performed by first excluding outlier pixels of features and background regions by flagging. The net Cy3 and Cy5 signal intensities for each feature were formed by subtracting the mean of the pixels in the local background from the mean of the pixels in the feature. Considering the features as the real indicators of expression, the spots were included whose foreground signals were significantly greater than the local background signals and additionally, $g(r)$ backgrounds were greater than 2.6 $g(r)$ background standard

deviation. Any differences in dye signal intensity were normalized using LOWESS method and a reliable log ratio, p-value and log ratio error for each feature was calculated to give a confidence measure that a gene has been differently expressed. The Onto-Express (OE) software and Annotation Database were used to analyze biology processes and annotate genes for the result of microarray, respectively.

Validation of microarray results by Real time qPCR

cDNAs were reverse transcribed from total RNA extracted from HCMV AD169 infected and uninfected ECV304 cells. The cDNAs were amplified by PCR with random six mers and the mixture containing 1×ExScript™ buffer, 5µM of dNTP mixture, 100 µM of Random 6 mers, 50 U of ExScript™ RTase, 10 U of RNase Inhibitor, 400 ng of total RNA and RNase Free dH₂O were carried out under the following conditions: 10 min at 42°C, 2 s at 95°C. Real-time qPCR was used to validate microarray and performed on a Rotor Gene 3000 Fluorescence quantitative detection system (CORBETT, Australia) using SYBR RT-PCR Kit DDR041A (Takara, Japan). PCR reactions in a final volume of 10µl reaction mixture contain 5µl PCR mixture, 1µl diluted cDNA and 0.5 iM each primer specific primers for six genes selected from differentially expressing genes. The PCR reactions were carried out under the following conditions: an initial denaturation of 5 min at 95°C; 45 cycles, each cycle consisting of 15 s at 95°C, 10 s at 60°C, and 15 s at 72°C. The detail information of special°C primers are showed in Table 1. At the end of the program, the specificity of the primer set was confirmed by melting curve analysis (65-95°C with a heating rate of 0.5°C/min). The copy numbers of target genes and GAPDH mRNA were estimated by comparing the results of real-time PCR with several dilutions (10², 10³, 10⁴, 10⁵, 10⁶, 10⁷ copies/reaction). The mRNA level of GAPDH was used to normalize the expression ratio of each gene.

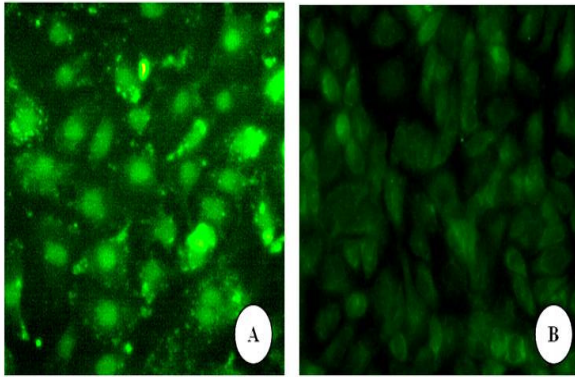
Analysis of HCMV infection process by Gene-Ontology and Gene Annotation

According to the biological process defined by Gene Ontology (GO) (<http://www.geneontology.org/>), Onto-Express software (OE) (<http://vortex.cs.wayne.edu/>) was used for analysis of differential expressed genes in HCMV-infected ECV304 cells. Database V2.0 (<http://www.genetools.microarray.ntnu.no/>) provides information from UniGene (NCBI), EntrezGene, SwissProt and Gene Ontology (GO), which were used

Results

HCMV infection in ECV304 cells

The pp65 is used for rapid diagnosis of infected-host cells, which is expressed in the host cell nuclei during the early phase of the replication cycle (Ho et al, 1998). In this study, we evaluated the expression of pp65 in ECV304 cells using immunofluorescence that is simple, reliable, less time-consuming and cheap. ECV304 cells were infected with HCMV AD169 strain as described in the methods reported for this study. Cells infected with HCMV AD169 showed very intense nuclear staining (figure 1A). In contrast, uninfected cells displayed no detectable staining if subjected to the same conditions as infected cells (figure 1B). In addition, the size of PCR products of HCMV IE gene is consistent to prediction (figure 2). These results indicated that HCMV AD169 stain could infect ECV304 cells.



Detection of HCMV pp65 IE protein in HCMV-infected ECV304 cells using immunofluorescence and PCR ECV304 cells were infected with HCMV AD169 strain as described in the methods reported for this study.

A: Infected group at 4 d post-infection (green fluorescence show positive pp65 protein locate in infected cells), **B:** Uninfected group (Original magnification 400×).

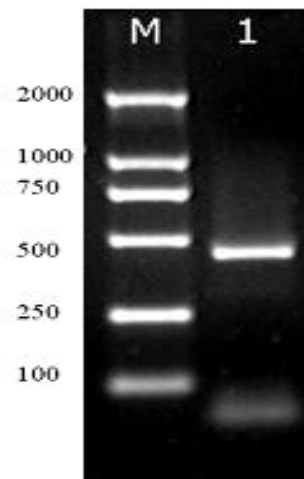


Figure 2: Detection of HCMV pp65 IE protein in HCMV-infected ECV304 cells using immunofluorescence and PCR

Confirmation of total RNA quality

The agar gel electrophoresis showed that there were three bands of 28S rRNA, 18S rRNA and 5S rRNA, with light degradation and little DNA contamination, meeting DNA microarray requirements

Quality control of microarray hybridization

The data is evaluated using Agilent G2567AA Feature Extraction Software (version 7.1) for hybridization efficiency and specificity. The effective hybrid spots were more than 99% meeting the requirements of analysis. As shown in figure 3, the background signal was low. The hybridization signal was homogenous and the shape was regular.

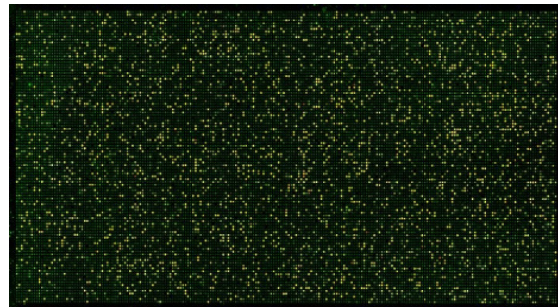


Figure 3: Microarray hybridization scanning picture

The scatter plots of hybridizing signal

The fluorescence intensity of the chip was analyzed using scatter plots. The scatter plot of fluorescence intensities from all points was drawn with gProcessedsignal (Cy3) as ordinate against rProcessedsignal (Cy5) as abscissa as indicated in figure 4). Three colours were used to stand for the distribution of two fluorescence signals from all hybrid dots. The yellow dots represent no significant difference between gProcessedsignal and rProcessedsignal, while red and blue represent significant difference between them. In addition, The red dots indicated upregulated genes of ECV304 cells and the blue dots indicated downregulated genes. According to the distribution of fluorescence intensities, most of the dots were distributed in the yellow region with a few red and blue dots, which is consist with the general rule of high-density cDNA microarray hybridization.

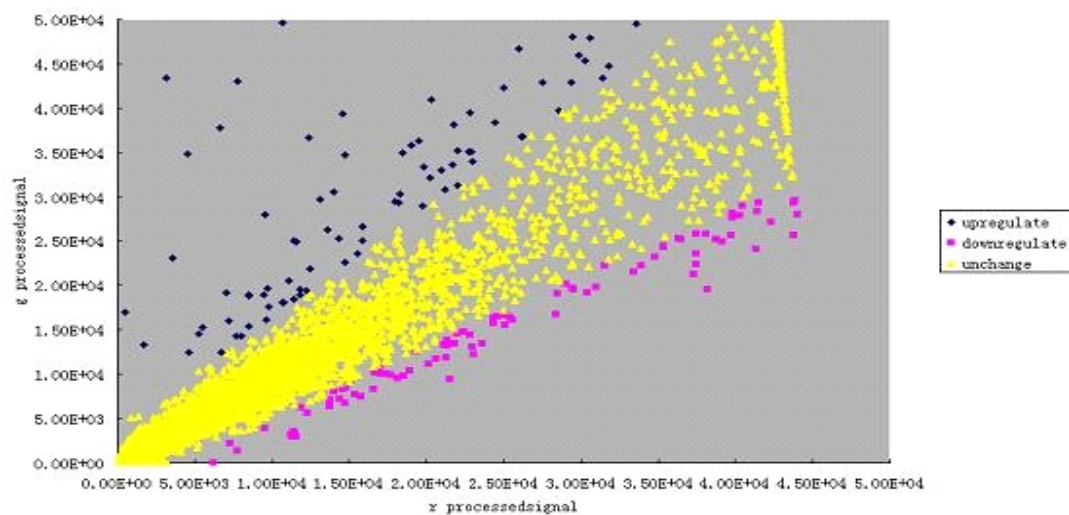


Figure 4: Scatter plot of Cy3/Cy5 hybridization intensity in microarray

The fluorescence intensity of the chip was analyzed using scatter plots. The scatter plot of fluorescence intensities from all points was drawn with gProcessedsignal (Cy3) as ordinate against rProcessedsignal (Cy5) as abscissa.

Table 1: Sequence information of primers designed

Gene Name	GenBank Accession No.	Gene name	Sequence	GG(%)	Tm (°C)	Size (bp)
GAPDH	NM_002046	Homo sapiens glyceraldehyde-3-phosphate dehydrogenase (GAPDH), mRNA.	F:- GCACCGTCAAGGCTGAGAAC	60	63.29	142
			R:-ATGGTGGTGAAGACGCCAGT	55	62.9	
RPS24	NM_033022	Homo sapiens ribosomal protein S24 (RPS24), transcript variant 1, mRNA	F:-GACAACCTGGCTTTGGCATGATTTA	41.6	64.37	174
			R:-CCA ACATTGGCCITTTGCAGTC	52.3	64.96	
LRRC28	NM_144598	Homo sapiens leucine rich repeat containing 28 (LRRC28), mRNA.	F:-GTTTGCCCAAGAAATTGGTCGTC	50	64.95	190
			R:-GGTCCACAGTGAGGTACTGCAGAG	58.3	64.58	
MGC8721	NM_016127	Homo sapiens hypothetical protein MGC (MGC8721), mRNA	F:-TTCCACCGTTACCAGAGATTCA	47.8	64.92	179
			R:-CAGTTCCTCAAGCCTGTCCAGA	57.1	64.87	
SLC3	NM_024330	Homo sapiens solute carrier family 27, member 3 (SLC3), mRNA.	F:-AGGTGCTGGAGACATATGGACTGAC	52	64.92	142
MST4	NM_016542	Homo sapiens Mst3 and SOK1-related kinase (MST4), mRNA	F:-AATACCTGGGCGGTGGTTCA	55	64.72	74
			R:-CATGGTAGCAATCTGGAACATCA	44	64.5	
TRAF2	NM_021138	Homo sapiens TNF receptor-associated factor 2 (TRAF2), mRNA.	F:-GGACCAAGCTGGAAGCCAAGTA	54.5	64.84	165
			R:-CTTCATATATGCCCTCGTGAACACA	44	64.27	

Differential expressed gene in HCMV infected-ECV304 cells

The result showed that there were 559 differential expressed genes. 471 genes were found to be expressed up-regulated; 334 of which had clear functions, while 88 genes were found to be expressed down-regulated, 69 of which had clear functions (table 2 and 3). Fold difference is the differences in multiples between HCMV infected-ECV304 cells and uninfected cells. Positive values described up-regulation while negative values described down-regulation.

Table 2: List of up-regulated genes during HCMV infection in ECV304 cells

GeneName	Fold difference	GeneName	Fold difference	GeneName	Fold difference	GeneName	Fold difference	GeneName	Fold difference
MGC2668	16.83	FLJ20446	7.39	CNR1	5.84	LOC90355	4.64	FRDA	3.39
FLJ22757	12.59	TA-LRRP	7.39	ZFP1	5.83	LHFP	4.58	SPAG6	3.38
GDNF	11.94	FGFR2	7.37	CYP11	5.71	POMZP3	4.54	KCNK2	3.32
EHF	11.61	PPARA	7.31	ABCA8	5.71	ART1	4.51	PLA7	3.32
TECTB	11.38	STAG1	7.20	HD	5.62	CISH	4.37	SEPX1	3.24
STAR	10.99	FLJ35808	7.11	CACNA2D1	5.60	ASAH2	4.33	TM9SF2	3.22
ATSV	10.73	DSCR10	7.08	KREMEN1	5.56	SLC2	4.32	CRB1	3.17
NFIB	10.53	B3GNT7	6.96	MGC21854	5.49	PCTP	4.21	DCOHM	3.15
HEAB	10.53	FLJ90440	6.93	MT1H	5.35	MST4	4.03	MRPS	3.14
GSTM1	10.07	BM039	6.87	CPO	5.31	HSD17B2	3.98	HMG20B	3.12
QDPR	9.49	C2GNT3	6.76	RGC32	5.26	CTPS2	3.90	GRIK3	3.11
DEFB127	9.46	MGC1203	6.75	HTR7	5.26	MGC10974	3.87	DPM2	3.10
BET1	9.44	FLJ21865	6.73	KIAA0570	5.22	ENO3	3.85	BCL10	3.08
TNFSF9	9.02	ALS2CR2	6.63	KRTAP9-2	5.11	COPI	3.85	USP13	3.08
CYB5R1	8.74	CAPG	6.62	C20orf96	5.09	IGLL1	3.84	UNC5H2	3.06
FLJ20174	8.63	FLJ13204	6.54	SLC6	5.08	DKFZp131	3.83	ATP6V2	3.06
SH2D	8.23	CYP1	6.29	CRKL	5.00	CAPNS2	3.68	RPS6KA5	3.05
SPIB	8.07	ARHGAP15	6.23	ZFP2	4.87	SLC22	3.67	VLCS-H1	2.99
HSPC023	8.07	MGC49942	6.07	FLJ90311	4.86	GPD1	3.64	PRTN3	2.98
LGALS8	7.95	SMARCA2	6.06	TCFL5	4.83	MBD2	3.64	SNFT	2.98
KCNMB1	7.89	RB1CC1	6.05	TM4SF5	4.80	SMARCA3	3.62	C1orf1	2.98
TGFBRAP1	7.66	SNTB2	6.04	CNTN5	4.79	PPIF	3.61	ITGA5	2.97
SEC24B	7.64	FLJ23360	5.93	MUT	4.78	CHRNA10	3.58	MGC5528	2.96
MGC3295	7.50	FOXL1	5.93	UGT2B11	4.75	LY64	3.52	MPG	2.96
WBCSR5	7.41	NICE-4	5.89	FLJ14909	4.64	CST5	3.43	ABCC3	2.95

Table 2 Continued

Gene Name	Fold difference	GeneName	Fold difference	GeneName	Fold difference	GeneName	Fold difference	GeneName	Fold difference
FLJ23168	1.71	MGC15397	1.60	GIT1	1.48	CDH11	1.40	NM_138456.2	6.68
UNC45	1.71	HTR	1.60	KIF	1.48	PAPPA	1.39	I_961848	6.57
FLJ11785	1.70	LENG5	1.59	SGCE	1.48	TNP1	1.39	I_963496	6.32
CHGA	1.70	NRP2	1.59	HAVCR1	1.48	LOX	1.39	NM_178470.1	6.14
CCNE2	1.68	EXO1	1.58	ARHGEF1	1.48	RBP3	1.38	NM_173686.1	5.81
LOC51142	1.68	TNNC2	1.58	MIP	1.47	HOXA11	1.38	I_1100065	5.79
MAGEA3	1.68	NELL1	1.58	TBX2	1.47	IDI1	1.37	I_963989	5.61
DDX18	1.66	HIST1H2BF	1.58	PACRG	1.47	FTH1	1.37	NM_001455.1	5.22
CD2AP	1.66	SYNPR	1.58	MNT	1.46	MGC16386	1.37	NM_138820.1	5.21
MYO	1.65	GEMIN7	1.58	PAPSS2	1.46	NM_152669.1	50.10	I_1000218	4.99
MGC40499	1.65	NANS	1.57	ALEX3	1.46	I_959644	16.61	NM_014693.1	4.94
RAB31	1.65	CARD15	1.57	LAMC1	1.45	I_1846457.FL1	13.81	NM_153263.1	4.87
TCFL4	1.64	FLJ23259	1.56	MGC3207	1.45	NM_152494.1	11.84	NM_005450.1	4.80
BRE	1.64	MARS	1.56	MGC14161	1.44	NM_015018.1	11.52	I_1000397	4.79
DKFZp434E2220	1.64	DMRTC2	1.56	FLJ20637	1.43	I_1109448	11.35	I_1109096	4.78
MICB	1.64	KIAA0700	1.55	GNB1	1.43	NM_144664.1	11.10	NM_144679.1	4.66
C22orf20	1.63	PLA	1.55	RPS6KL1	1.43	I_962816	10.38	I_951081	4.38
CALM2	1.63	VAPB	1.55	ADAMTS5	1.43	I_963159	9.84	I_1151919	4.13
HOXD10	1.63	PVRL3	1.54	FLJ22794	1.42	I_1000440	9.19	NM_153030.1	4.06
CCNDBP1	1.62	NOS1	1.53	CHAF1B	1.42	NM_153010.3	9.10	I_1985061.FL1	3.97
GPR10	1.62	TXNIP	1.51	MGC13125	1.41	I_963100	8.88	I_964564	3.66
SFXN2	1.61	FLJ20605	1.50	DKFZP434P1750	1.41	I_1110275	8.86	NM_152684.1	3.63
CYP2	1.61	ATP6V2	1.50	LOC51239	1.41	I_963013	7.79	I_944014	3.63
PTK	1.61	BTAF1	1.50	C12orf8	1.40	I_960313	7.60	I_931201	3.56
CYP27B1	1.60	BAG3	1.49	KRTAP9-4	1.40	NM_152360.1	7.48	I_965874	3.56

Gene Name	Fold difference	GeneName	Fold difference	GeneName	Fold difference	GeneName	Fold difference	GeneName	Fold difference
FLJ23168	1.71	MGC15397	1.60	GIT1	1.48	CDH11	1.40	NM_138456.2	6.68
UNC45	1.71	HTR	1.60	KIF	1.48	PAPPA	1.39	I_961848	6.57
FLJ11785	1.70	LENG5	1.59	SGCE	1.48	TNP1	1.39	I_963496	6.32
CHGA	1.70	NRP2	1.59	HAVCR1	1.48	LOX	1.39	NM_178470.1	6.14
CCNE2	1.68	EXO1	1.58	ARHGEF1	1.48	RBP3	1.38	NM_173686.1	5.81
LOC51142	1.68	TNNC2	1.58	MIP	1.47	HOXA11	1.38	I_1100065	5.79
MAGEA3	1.68	NELL1	1.58	TBX2	1.47	IDI1	1.37	I_963989	5.61
DDX18	1.66	HIST1H2BF	1.58	PACRG	1.47	FTH1	1.37	NM_001455.1	5.22
CD2AP	1.66	SYNPR	1.58	MNT	1.46	MGC16386	1.37	NM_138820.1	5.21
MYO	1.65	GEMIN7	1.58	PAPSS2	1.46	NM_152669.1	50.10	I_1000218	4.99
MGC40499	1.65	NANS	1.57	ALEX3	1.46	I_959644	16.61	NM_014693.1	4.94
RAB31	1.65	CARD15	1.57	LAMC1	1.45	I_1846457.FL1	13.81	NM_153263.1	4.87
TCFL4	1.64	FLJ23259	1.56	MGC3207	1.45	NM_152494.1	11.84	NM_005450.1	4.80
BRE	1.64	MARS	1.56	MGC14161	1.44	NM_015018.1	11.52	I_1000397	4.79
DKFZp434E2220	1.64	DMRTC2	1.56	FLJ20637	1.43	I_1109448	11.35	I_1109096	4.78
MICB	1.64	KIAA0700	1.55	GNB1	1.43	NM_144664.1	11.10	NM_144679.1	4.66
C22orf20	1.63	PLA	1.55	RPS6KL1	1.43	I_962816	10.38	I_951081	4.38
CALM2	1.63	VAPB	1.55	ADAMTS5	1.43	I_963159	9.84	I_1151919	4.13
HOXD10	1.63	PVRL3	1.54	FLJ22794	1.42	I_1000440	9.19	NM_153030.1	4.06
CCNDBP1	1.62	NOS1	1.53	CHAF1B	1.42	NM_153010.3	9.10	I_1985061.FL1	3.97
GPR10	1.62	TXNIP	1.51	MGC13125	1.41	I_963100	8.88	I_964564	3.66
SFXN2	1.61	FLJ20605	1.50	DKFZP434P1750	1.41	I_1110275	8.86	NM_152684.1	3.63
CYP2	1.61	ATP6V2	1.50	LOC51239	1.41	I_963013	7.79	I_944014	3.63
PTK	1.61	BTAF1	1.50	C12orf8	1.40	I_960313	7.60	I_931201	3.56
CYP27B1	1.60	BAG3	1.49	KRTAP9-4	1.40	NM_152360.1	7.48	I_965874	3.56

Table 2 Continued

GeneName	Fold difference	GeneName	Fold difference	GeneName	Fold difference	GeneName	Fold difference
I_962880	3.53	NM_178034.1	2.34	I_965027	1.82	NM_016590.2	1.53
NM_033416.1	3.41	I_957174	2.32	I_1109565	1.81	I_948919	1.52
NM_175053.1	3.40	I_962558	2.29	I_963639	1.77	I_958442	1.52
NM_178840.1	3.27	I_964457	2.26	I_931895	1.76	I_936605	1.52
I_1912044.FL1	3.07	I_1109311	2.23	I_928385	1.76	I_959893	1.51
NM_003017.2	2.97	I_930224	2.21	I_1918165.FL1	1.75	NM_005205.2	1.51
I_939261	2.93	I_960356	2.18	NM_138817.1	1.75	I_1100871	1.50
I_2015145.FL2	2.90	NM_005737.2	2.17	I_966202	1.72	I_962912	1.48
I_1001950	2.89	I_1109914	2.15	I_958498	1.68	NM_176811.1	1.48
I_931549	2.84	NM_175906.1	2.14	I_959040	1.68	I_930598	1.48
I_928342	2.76	I_2020917.FL1	2.07	I_962848	1.67	NM_153184.1	1.47
I_962649	2.72	I_928994	2.07	I_1109458	1.67	I_1109420	1.47
I_961465	2.71	NM_175745.1	2.05	I_957145	1.66	I_1109342	1.46
I_936604	2.71	NM_152420.1	2.03	I_1847600.FL1	1.66	NM_174900.1	1.45
NM_152768.1	2.70	I_930338	2.03	I_961307	1.65	I_930237	1.45
NM_032721.2	2.69	NM_001130.4	1.99	NM_002648.1	1.65	I_1109691	1.44
I_962007	2.66	I_1100234	1.97	NM_138422.1	1.65	I_1100108	1.44
I_929707	2.66	I_965124	1.94	I_1109345	1.63	I_950247	1.41
I_965788	2.63	I_956871	1.90	I_931079	1.62	NM_153235.1	1.38
NM_178503.1	2.60	I_1958495.FL1	1.90	I_1000606	1.62	I_966412	1.37
I_1109303	2.59	NM_080662.1	1.88	I_958063	1.57	I_963553	1.37
NM_152371.1	2.59	I_957754	1.86	I_1151935	1.54		
NM_178545.1	2.56	NM_148895.1	1.85	I_929587	1.54		
NM_175918.1	2.53	NM_018338.1	1.84	I_1152052	1.53		
NM_139166.1	2.48	I_931318	1.84	I_963177	1.53		

Table 3: List of down-regulated genes during HCMV infection in ECV304 cells

GeneName	Fold difference	GeneName	Fold difference	GeneName	Fold difference	GeneName	Fold difference
UEV3	-131.19	UBN1	-1.75	LOC92906	-1.54	I_1100727	-3.41
LRRC28	-5.88	PRM1	-1.75	PTCH	-1.54	I_1109316	-1.92
EBAG9	-3.99	GNE	-1.75	TTC1	-1.54	I_954745	-1.90
ALLC	-3.86	HS747E	-1.74	NR1H2	-1.52	I_1109663	-1.81
DYRK1B	-3.85	FLJ34389	-1.72	CYP4X1	-1.52	I_1100463	-1.76
CDKL5	-3.74	AGC1	-1.72	NM_004128.1	-1.51	I_1109571	-1.75
NM_152466.1	-3.49	FBN1	-1.71	SLC8	-1.51	I_1151840	-1.59
C8B	-3.48	H326	-1.70	NM_152680.1	-1.51	I_3260602.FL1	-1.57
OR1	-3.23	PCDHB3	-1.70	C21orf62	-1.50	I_965931	-1.56
FACL4	-2.42	TNFSF10	-1.67	MAGEA6	-1.50	I_958455	-1.54
FLJ34658	-2.21	RNF2	-1.66	COX2	-1.49	I_1201909	-1.49
NM_152693.1	-2.20	FAM1	-1.64	GPR74	-1.49	I_1001952	-1.49
CAP350	-2.15	HDAC5	-1.63	LYL1	-1.49	I_960767	-1.42
MGC33212	-2.13	KRT1	-1.62	CGI-30	-1.48		
MGC15737	-2.00	RGS2	-1.61	GCKR	-1.46		
ALG12	-2.00	SIGIRR	-1.61	NM_025049.1	-1.46		
DDX11	-1.99	SNAPAP	-1.60	KIAA0372	-1.45		
RPL24	-1.96	CD7	-1.58	IL7	-1.45		
FAM	-1.91	SSBP3	-1.58	C1orf27	-1.44		
MGC4293	-1.91	MEL	-1.58	B4GALT1	-1.44		
MGC33214	-1.88	RGS6	-1.57	IRTA1	-1.44		
FLJ20551	-1.81	DGUOK	-1.57	PSMF1	-1.44		
UPF3B	-1.80	TFB	-1.55	GPCR1	-1.42		
GIOT-3	-1.79	LOC112840	-1.55	DAPK2	-1.42		
MRPL30	-1.76	ZNF93	-1.54	NM_004252.1	-1.41		

Validation of microarray results

Six gene selected was performed using real-time RT-PCR to validate microarray results and relative quantitation results was showed as follow (table 4). Genes determined by real-time RT-PCR showed

similar patterns of expression to those analyzed by microarray, suggesting data reliability from cDNA microarray that settle the base for bio-information analysis and study on the function.

Table 4: Relative quantitation results of real time RT-PCR

Target Gene Name		IS(GADPH)		Target Gene		Relative quantitaion (Z)	array (Ratio**)	difference (Z-Ratio)
		Result of quantitaion (copies*)	Relative quantitaion (X)	Relative quantitaion (Y) (copies*)	Adjustive quantitaion (Y/X) (copies*)			
RPS24	control	16238723	1	60139368	60139368	1	2.44	/
	infection group	8862281	0.54	81432414	149211979	2.48		0.04
MGC8721	control	16238723	1	16839583	16839582	1	2.9	/
	infection group	8862281	0.54	26001917	47644388	2.83		-0.07
SLC3	control	16238723	1	451805	451805	1	2.24	/
	infection group	8862281	0.54	1217584	2231029	4.94		2.70
MST4	control	16238723	1	451805	451805	1	4.03	/
	infection group	8862281	0.54	1425852	2612647	5.78		1.75
TRAF2	control	16238723	1	1488105	1488105	1	2.67	/
	infection group	8862281	0.54	3049637	5587975	3.76		1.09
LRRC28	control	16238723	1	11469841	11469841	1	0.17	/
	infection group	8862281	0.54	1272521	2331692	0.20		0.03

Biological process analysis of HCMV infection process

559 differential expressed genes were involved in 273 biological processes, 39 of which were significant ($P < 0.05$). As shown in table 5, information from UniGene(NCBI), EntrezGene and Gene Ontology (GO) were used for function annotation and analysis of genes in HCMV infection process. Differential expressed genes induced by HCMV infection were also involved in the pathogenic mechanism of HCMV infection. These genes included apoptosis-related genes (Granzyme B, DAPK2, TARF2, TNFSF9, TNFSF10, Bcl-2L10, TGFBRAP1), G-protein-coupled receptors signal transduction pathway-related genes (RGS6, RGS2, GIT1), c-jun

N-terminal kinase and MAPK signaling pathway-related genes (CRKL, SH2D3A, MAP2K2), cell cycle-related genes (cyclinE, E2F), cancer-related genes (MYCL-2). In these biological processes, the P value of signal transduction-related genes is lowest ($P = 0.005$), containing 21 genes. DNA-dependent transcriptional regulation-related genes were the most, containing 29 genes.

Table 5: Results of Biological process analysis of HCMV Infection process by Gene-Ontology and Gene Annotation

Biological Process	Gene name	Entrez Gene	UniGene ID	P-Value
1. signal transduction				0.005
	N-acylsphingosine amidohydrolase (non-lysosomal ceramidase) 2	56624	Hs.512645	
	CD2-associated protein	23607	Hs.485518	
	Arginine vasopressin receptor 1B	553	Hs.1372	
	Prolactin releasing hormone receptor	2834	Hs.248119	
	Chemokine (C-X-C motif) receptor 3	2833	Hs.198252	
	Vascular endothelial growth factor	7422	Hs.73793	
	Cannabinoid receptor 1 (brain)	1268	Hs.75110	
	Guanine nucleotide binding protein (G protein), beta polypeptide 1	2782	Hs.430425	
	Brain and reproductive organ-expressed (TNFRSF modulator)	9577	Hs.258314	
	Growth hormone releasing hormone receptor	2692	Hs.767	
	Glial cell derived neurotrophic factor	2668	Hs.248114	
	Patched homolog (Drosophila)	5727	Hs.494538	
	Tumor necrosis factor (ligand) superfamily, member 9	8744	Hs.1524	
	Tumor necrosis factor (ligand) superfamily, member 10	8743	Hs.478275	
	5-hydroxytryptamine (serotonin) receptor 7 (adenylate cyclase-coupled)	3363	Hs.73739	
	5-hydroxytryptamine (serotonin) receptor	3355	Hs.248136	
	TNF receptor-associated factor 2	7186	Hs.522506	
	Taste receptor, type 2, member 1	50834	Hs.567492	
	Membrane-spanning 4-domains, subfamily A, member 1	931	Hs.438040	
	G protein-coupled receptor 74	7265	Hs.519718	
	Ribosomal protein S6 kinase, 90kDa, polypeptide 5	9252	Hs.510225	
2. regulation of transcription, DNA-dependent				0.044
	Forkhead	2300	Hs.533830	
	Transcription factor-like 5 (basic helix-loop-helix)	10732	Hs.30696	
	Chromosome 17 open reading frame 49	124944	Hs.511801	
	Ring finger protein 2	6045	Hs.124186	
	Single stranded DNA binding protein 3	23648	Hs.547759	
	Regulatory factor X, 4 (influences HLA class II expression)	5992	Hs.388827	
	Interferon regulatory factor 5	3663	Hs.521181	
	Hypothetical protein FLJ14981	84954	Hs.321689	
	Chromatin assembly factor 1, subunit B (p60)	8208	Hs.75238	
	MAX binding protein	4335	Hs.253552	
	Nuclear receptor subfamily 1, group H, member 2	7376	Hs.432976	
	SWI/SNF related, matrix associated, actin dependent regulator of chromatin, subfamily a, member 3	6596	Hs.3068	
	Bromodomain adjacent to zinc finger domain,	11177	Hs.509140	
	High-mobility group 20B	10362	Hs.406534	
	E transcription factor 2	1870	Hs.194333	
	Jun dimerization protein p21SNFT	55509	Hs.62919	
	DMRT-like family C2	63946	Hs.350507	
	Lymphoblastic leukemia derived sequence 1	4066	Hs.46446	
	Nuclear factor I/B	4781	Hs.370359	
	Homeo	3236	Hs.123070	
	Homeo	3207	Hs.249171	
	Cyclin H	902	Hs.292524	
	Peroxisome proliferative activated receptor, alpha	5465	Hs.534037	
	Ribosomal protein S6 kinase, 90kDa, polypeptide 5	9252	Hs.510225	
	Histone deacetylase 5	10014	Hs.438782	
	MAX-like protein X	6945	Hs.383019	
	T-box 2	6909	Hs.531085	

Continuation of table 5

Biological Process	Gene name	Entrez Gene	UniGene ID	P-Value
3. cleavage of lamin	Granzyme B (granzyme 2, cytotoxic T-lymphocyte-associated serine esterase 1)	3002	Hs.1051	0.03
4. histidine catabolism	Histidine ammonia-lyase	3034	Hs.190783	0.039
5. response to chemical substance	Ribosomal protein S6 kinase, 90kDa, polypeptide 5	9252	Hs.510225	0.027
6. regulation of angiogenesis	Keratin 1 (epidermolytic hyperkeratosis)	3848	Hs.80828	0.029
7. positive regulation of vascular endothelial growth factor receptor signaling pathway	Vascular endothelial growth factor	7422	Hs.73793	0.034
8. response to freezing	N-acetylneuraminic acid synthase (sialic acid synthase)	54187	Hs.522310	0.019
9. lipopolysaccharide biosynthesis	N-acetylneuraminic acid synthase (sialic acid synthase)	54187	Hs.522310	0.045
	Glucosamine (UDP-N-acetyl)-2-epimerase/N-acetylmannosamine kinase	10020	Hs.5920	
10. lactate transport	Solute carrier 16 (monocarboxylic acid transporters), member 8	23539	Hs.270285	0.03
11. UDP-N-acetylglucosamine metabolism	Glucosamine (UDP-N-acetyl)-2-epimerase/N-acetylmannosamine kinase	10020	Hs.5920	0.028
12. dihydrobiopterin metabolism	Quinoid dihydropteridine reductase	5860	Hs.75438	0.038
13. DNA replication-dependent nucleosome assembly	Chromatin assembly factor 1, subunit B (p60)	8208	Hs.75238	0.048
14. cold acclimation	N-acetylneuraminic acid synthase (sialic acid synthase)	54187	Hs.522310	0.021
15. sulfate assimilation	3'-phosphoadenosine 5'-phosphosulfate synthase 2	9060	Hs.524491	0.028
16. neuromuscular junction development	CUG triplet repeat, RNA binding protein 2	10659	Hs.309288	0.045
17. lysyl-tRNA aminoacylation	Lysyl-tRNA synthetase	3735	Hs.3100	0.018
18. homeiothermy	N-acetylneuraminic acid synthase (sialic acid synthase)	54187	Hs.522310	0.024
19. detection of abiotic stimulus	G protein-coupled receptor 74	10886	Hs.99231	0.049
20. carotenoid biosynthesis	Isopentenyl-diphosphate delta isomerase 1	3422	Hs.283652	0.036
21. protein repair	Selenoprotein X, 1	51734	Hs.279623	0.05
22. endoderm development	Laminin, gamma 1 (formerly LAMB2)	3915	Hs.497039	0.044
23. DNA dealkylation	N-methylpurine-DNA glycosylase	4350	Hs.459596	0.04
24. aging	Lysyl oxidase-like 2	4017	Hs.571480	0.048

Continuation of table 5

Biological Process	Gene name	Entrez Gene	UniGene ID	P-Value
25.platelet activating factor biosynthesis	Phospholipase A2, group IVA (cytosolic, calcium-dependent)	5321	Hs.497200	0.037
26.epithelial cell differentiation	Ets homologous factor	26298	Hs.502306	0.047
27.spermatid nuclear elongation	Transition protein 1 (during histone to protamine replacement)	7141	Hs.3017	0.022
28. estrogen metabolism	UDP glucuronosyltransferase 2 family, polypeptide B11	10720	Hs.339811	0.045
29.methionyl-tRNA aminoacylation	Methionine-tRNA synthetase	4141	Hs.355867	0.035
30.fertilization, exchange of chromosomal proteins	Transition protein 1 (during histone to protamine replacement)	7141	Hs.3017	0.033
31.S phase of mitotic cell cycle	DEAD/H (Asp-Glu-Ala-Asp/His) box polypeptide 11 (CHL1-like helicase homolog, <i>S. cerevisiae</i>)	1663	Hs.443960	0.027
32.complement activation, lectin pathway	Keratin 1 (epidermolytic hyperkeratosis)	3848	Hs.80828	0.042
33. leucine catabolism	Methylcrotonoyl-Coenzyme A carboxylase 2 (beta)	64087	Hs.167531	0.046
34.N-acetylneuraminic acid metabolism	Glucosamine (UDP-N-acetyl)-2-epimerase/N-acetylmannosamine kinase	10020	Hs.5920	0.017
35.peptidyl-diphthamide biosynthesis from peptidyl-histidine	DPH5 homolog (<i>S. cerevisiae</i>)	51611	Hs.440776	0.032
36. DNA damage induced protein phosphorylation	Ribosomal protein S6 kinase, 90kDa, polypeptide 5	9252	Hs.510225	0.046
37. icosanoid metabolism	Phospholipase A2, group IVA (cytosolic, calcium-dependent)	5321	Hs.497200	0.033
38.histone phosphorylation	Ribosomal protein S6 kinase, 90kDa, polypeptide 5	9252	Hs.510225	0.031
39. chromatin silencing	Transition protein 1 (during histone to protamine replacement)	7186	Hs.522506	0.041
	Histone deacetylase 5	10014	Hs.438782	

Discussion

cDNA microarray, which can simultaneously monitor the expression levels of thousands of genes to study the effects of certain treatments, diseases, and developmental stages on gene expression. cDNA microarray has been used to analyses of differential gene expression in virus-infected process, revealing the interaction of virus with host cells, exploring the pathogenic mechanisms of virus and developing antiviral drugs, which is an important research subject of viral infectomics¹⁵⁻¹⁷.

In 1998, Zhu et al¹⁸. firstly used DNA array technology to global monitor the levels of about 6600 human mRNAs in HCMV-infected cells as compared with uninfected ones. The level of 258 mRNAs changed by a factor of 4 or more before the onset of viral DNA replication. Several of these mRNAs encode gene products that might play key roles in virus-induced pathogenesis. So it is important to identify them as intriguing targets for further study. In previous study, they used differential display

analysis to assess the effect of HCMV infection on the accumulation of cellular RNAs. Fifty-seven partial cDNA clones were isolated, representing about 26 differentially expressed mRNAs. 11 of these mRNAs were virus-coded, and 15 were of cellular origin. But the detection throughout and sensitivity using differential display analysis were lower than those from DNA microarray technology^{18, 19}. Browne et al¹¹. used gene chip technology to analyze the effect of HCMV infection on cellular mRNA accumulation and 1425 cellular mRNAs, which include cell cycle regulators, apoptosis regulators, inflammatory pathway genes and immune regulators, were found to be up-regulated or down-regulated by threefold or greater. Simmen et al¹². showed that HCMV-regulated gene expression profile in fibroblasts using high-density cDNA microarrays and found that the interaction of gB with its as yet unidentified cellular receptor is the principal mechanism by which HCMV alters cellular gene expression early during infection. These results suggested that HCMV could affect the expression of host genes through many mechanisms. However, most studies just focused on human fibroblast as the host cell infected by HCMV.

In this study, we used ECV304 as target cells to global monitor the effect of HCMV on ECV304 gene expression profiling using 60-mer high-density oligo microarra. ECV304 was reported first in 1990 as a spontaneously - transformed and immortalized cell line, which derived from a Japanese HUVEC²⁰. It is a permanent endothelial cell line and has been used widely as an endothelial cell model and a useful research tool in biomedicine and pharmacology. The result showed that there were 559 differential expressed genes. 471 genes were found to be expressed up-regulated, 334 of which had clear functions, while 88 genes were found to be expressed down-regulated, 69 of which had clear functions. These genes which included apoptosis-related genes, G-protein-coupled receptors signal transduction pathway-related genes, c-jun N-terminal kinase and MAPK signaling pathway-related genes, cell cycle-related genes and cancer-related genes. In these biological processes, signal transduction-related genes and DNA-dependent transcriptional regulation-related genes seem to be important in HCMV infection process. These genes were analyzed by microarray showed similar patterns of expression to those determined by real-time RT-PCR, suggesting data reliability from cDNA microarray that settle the base for bio-information analysis and

study on the function. A set of genes were identified as differential expression in this study and some of them might be associated with biological process of HCMV pathogenetic. These genes are elucidated as follows.

VEGF gene is a member of the PDGF/VEGF growth factor family and encodes a protein that is often found as a disulfide linked homodimer. This protein is a glycosylated mitogen that specifically acts on endothelial cells and has various effects, including mediating increased vascular permeability, inducing angiogenesis, vasculogenesis and endothelial cell growth, promoting cell migration, and inhibiting apoptosis. In our study, up-regulated VEGF gene might associate with some damage induced by HCMV as its function in cell biological process. RGS6 (regulator of G-protein signaling 6) and RGS2 (regulator of G-protein signaling 2), which are decode regulators of G protein and have been shown to modulate the functioning of G proteins by activating the intrinsic GTPase activity of the alpha (guanine nucleotide-binding) subunits. Signalling by G proteins is controlled by the regulator of G-protein signalling (RGS) proteins that accelerate the GTPase activity of Galpha subunits and act in a G-protein-coupled receptor (GPCR)-specific manner. Because GPCRs play a crucial role in cellular communication, and chemokine receptors are essential for leukocyte trafficking in particular. The virus-encoded GPCRs (vGPCRs) may be crucial determinants of viral pathogenesis²¹. Expression of vGPCRs may play a prominent role in immune evasion, promoting virus dissemination, or modulating cellular responses of infected cells. Within the HCMV genome, four genes encoding GPCRs have previously been identified (US27, US28, UL33, and UL78)²². On the basis of sequence alignments, it has been identified that HCMV may effectively use UL33 to orchestrate multiple signaling networks within infected cells.

TNFSF9 (Tumor necrosis factor (ligand) superfamily, member 9) and TNFSF10 (Tumor necrosis factor (ligand) superfamily, member 10), which encode the protein, are cytokines that belong to the tumor necrosis factor (TNF) ligand family. This cytokine encoded by TNFSF9 is a ligand for TNFRSF9/4-1BB, which is a costimulatory molecule in T lymphocytes. This cytokine and its receptor are involved in the antigen presentation process, and in the generation of cytotoxic T cells. It is found to express in various cancer cell lines, involve in T cell-tumor cell interaction, and also be required for the optimal CD8 responses in CD8 T cells. This protein

decoded by TNFSF10 preferentially induces apoptosis in transformed and tumor cells, but does not appear to kill normal cells although it is expressed at a significant level in most normal tissues. This protein binds to several members of TNF receptor superfamily including TNFRSF10A/TRAILR1, TNFRSF10B/TRAILR2, TNFRSF10C /TRAILR3, TNFRSF10D /TRAILR4, and possibly also to TNFRSF11B/OPG. The activity of this protein may be modulated by binding to the decoy receptors TNFRSF10C/TRAILR3, TNFRSF10D/TRAILR4, and TNFRSF11B/OPG that cannot induce apoptosis. The binding of this protein to its receptors has been shown to trigger the activation of MAPK8/JNK, caspase 8, and caspase 3. Our study showed the two genes were regulated by HCMV.

It was found that the biological process, such as S phase of mitotic cell cycle, was significant in HCMV infection. DEAD box proteins, characterized by the conserved motif Asp-Glu-Ala-Asp (DEAD), are putative RNA helicases. They are implicated in a number of cellular processes involving alteration of RNA secondary structure such as translation initiation, nuclear and mitochondrial splicing, and ribosome and spliceosome assembly. The protein decoded by DDX11 gene is most important component in regulation of mitotic cell cycle. DDX11 is a homolog of the yeast CHL1 gene, and may function to maintain chromosome transmission fidelity and genome stability. Based on their distribution patterns, some members of this family are believed to be involved in embryogenesis, spermatogenesis, and cellular growth and division²³. In our previous study, the change of S phase effected by the HCMV infection in ECV304 cells at four days post-infection was demonstrated. HCMV productively infect terminally differentiated cells of the host that are in the G0 phase of the cell cycle. Human foreskin fibroblast (HFF) cells are widely used for permissive HCMV infection in tissue culture. These cells withdraw from the cell cycle on contact inhibition and are in G0 arrest or G1 phase. Because HCMV do not encode many of the biosynthetic enzymes for DNA precursor synthesis, the virus requires a mechanism to overcome cellular quiescence. HCMV infection induces the progression of quiescent cells toward the G1_S transition point and activates cellular genes required for DNA replication such as thymidine kinase (TK)²⁴, dihydrofolate reductase (DHFR)²⁵, cyclin E²⁶ and DNA polymerase²⁷. Genes that are differentially expressed during infection can potentially provide insights into the complex regulatory phenomena at the transcriptional level

within ECV304 cells in response to HCMV infection. Up-regulated genes may represent host responses to stress stimuli and/or viral induced mechanisms of pathogenesis. On the other hand, the down-regulation of other cellular transcripts may be partially attributed to the shutoff of host macromolecular synthesis in favor of viral replication.

MAP2K2 (mitogen-activated protein kinase 2) can encode a protein, which is a dual specificity protein kinase belonging to the MAP kinase kinase family²⁸. This kinase is known to play a critical role in mitogen growth factor signal transduction. Subsequently it phosphorylates and thus activates MAPK1/ERK2 and MAPK2/ERK3. The activation of this kinase itself is dependent on the Ser/Thr phosphorylation by MAP kinase kinase kinases. The inhibition or degradation of this kinase is found to be involved in the pathogenesis of *Yersinia* and anthrax.

v-CRK avian sarcoma virus CT10-homolog-like (CRKL) contains one SH2 domain and two SH3 domains. CRKL has been shown to activate the RAS and JUN kinase signaling pathways and transform fibroblasts in a RAS-dependent fashion. It is a substrate of the BCR-ABL tyrosine kinase and plays a role in fibroblast transformation by BCR-ABL. In addition, CRKL has oncogenic potential.

MICA gene encodes the highly polymorphic MHC (HLA) class I chain-related gene A. The protein product is expressed on the cell surface, although unlike canonical class I molecules it does not seem to associate with beta-2-microglobulin. It is thought that MICA functions as a stress-induced antigen that is broadly recognized by intestinal epithelial gamma delta T cells. MICB gene encodes a heavily glycosylated protein which is a ligand for the NKG2D type II receptor. Binding of the ligand activates the cytolytic response of natural killer (NK) cells, CD8 alpha beta T cells, and gammadelta T cells which express the receptor. This protein is stress-induced and is similar to MHC class I molecules; however, it does not associate with beta-2-microglobulin or bind peptides. HCMV infection is associated with graft rejection by upregulating expression of MICA and MICB²⁹. Cyclin E decoded by CCNE1 gene belongs to the highly conserved cyclin family, whose members are characterized by a dramatic periodicity in protein abundance through the cell cycle. Cyclins function as regulators of CDK kinases. Different cyclins exhibit distinct expression and degradation patterns which contribute to the temporal coordination of each mitotic event. This

protein accumulates at the G1-S phase boundary and is degraded as cells progress through S phase. Overexpression of this gene has been observed in many tumors, which results in chromosome instability, and thus may contribute to tumorigenesis. Cyclin E/cdk2 kinase activity can be activated by the immediate-early genes, IE1 and IE2, in HCMV infected cells. Transactivation of the cyclin E promoter by IE2 has been reported³⁰, but the mechanism for IE1 activation of cyclin E/cdk2 kinase activity in HCMV-infected cells is still unclear. In this study, our experimental results are in agreement with the results obtained by Vierling et al.

BCL2L10 gene encodes a protein belonging to the BCL-2 protein family. BCL-2 family members form hetero- or homodimers and act as anti- or pro-apoptotic regulators that are involved in a wide variety of cellular activities. The protein encoded by this gene contains conserved BH4, BH1 and BH2 domains. This protein can interact with other members of BCL-2 protein family including BCL2, BCL2L1/BCL-X (L), and BAX. Overexpression of this gene has been shown to suppress cell apoptosis possibly through the prevention of cytochrome C release from the mitochondria, and thus activating caspase-3 activation. The mouse counterpart of this protein is found to interact with Apaf1 and forms a protein complex with Caspase 9, which suggests the involvement of this protein in APAF1 and CASPASE 9 related apoptotic pathway.

Conclusion

Among all biological processes induced by HCMV infection in ECV304 cells, the signal transduction-related genes were the most significant, which contained 21 genes, and those genes involved in various function in different signal transduction pathways. Though the roles of the cellular genes discussed above in HCMV replication and pathogenesis remain highly speculative, the ability to identify cellular genes whose functions provide tantalizing hints of potential mechanistic roles in infectious disease processes underscores the utility of cDNA microarray technology in the study of pathogens. The global analysis of changes in mRNA levels provides a catalog of genes that are modulated as a result of the host-pathogen interaction and therefore deserve further scrutiny. DNA array analysis provides an important new approach for the investigation of pathogenic mechanisms.

Acknowledgements

We thank Prof. WU Guo-jun Institute of Medical Microbiology, Central South University, China for kindly providing HCMV AD169 strain. This study was supported by The Science & Technology Foundation of Guizhou Province (No.[2007]2088).

References

1. Numazaki K. Congenital infection and HCMV. *Nihon Rinsbo* 2006; 64 Suppl 3: 496-499.
2. Streblov D N, Orloff S L, Nelson J A. Do pathogens accelerate atherosclerosis? *J Nutr* 2001; 131(10): 2798S-2804S.
3. Schottstedt V, Blumel J, Burger R, et al. Human Cytomegalovirus (HCMV) - Revised. *Transfus Med Hemother* 2010; 37(6): 365-375.
4. Melnick M, Sedghizadeh PP, Allen CM, et al. Human cytomegalovirus and mucoepidermoid carcinoma of salivary glands: cell-specific localization of active viral and oncogenic signaling proteins is confirmatory of a causal relationship. *Exp Mol Pathol* 2012; 92(1): 118-125.
5. Plachter B, Sinzger C, Jahn G. Cell types involved in replication and distribution of human cytomegalovirus. *Adv Virus Res* 1996; 46: 195-261.
6. Kahl M, Siegel-Axel D, Stenglein S, et al. Efficient lytic infection of human arterial endothelial cells by human cytomegalovirus strains. *J Virol* 2000; 74(16): 7628-7635.
7. Bissinger AL, Sinzger C, Kaiserling E, et al. Human cytomegalovirus as a direct pathogen: correlation of multiorgan involvement and cell distribution with clinical and pathological findings in a case of congenital inclusion disease. *J Med Virol* 2002; 67(2): 200-206.
8. Fish KN, Stenglein SG, Ibanez C, et al. Cytomegalovirus persistence in macrophages and endothelial cells. *Scand J Infect Dis Suppl* 1995; 99: 34-40.
9. Jarvis MA, Nelson JA. Human cytomegalovirus persistence and latency in endothelial cells and macrophages. *Curr Opin Microbiol*, 2002; 5(4): 403-407.
10. Jenner RG, Young RA. Insights into host responses against pathogens from transcriptional profiling. *Nat Rev Microbiol* 2005; 3(4): 281-294.
11. Browne E P, Wing B, Coleman D, et al. Altered cellular mRNA levels in human cytomegalovirus-infected fibroblasts: viral block to the accumulation

- of antiviral mRNAs. *J Virol* 2001; 75(24): 12319-12330.
12. Simmen KA, Singh J, Luukkonen B G, et al. Global modulation of cellular transcription by human cytomegalovirus is initiated by viral glycoprotein B. *Proc Natl Acad Sci U S A* 2001; 98(13): 7140-7145.
 13. Song Y J, Stinski M F. Effect of the human cytomegalovirus IE86 protein on expression of E2F-responsive genes: a DNA microarray analysis. *Proc Natl Acad Sci U S A*, 2002; 99(5): 2836-2841.
 14. Slobedman B, Stern J L, Cunningham AL, et al. Impact of human cytomegalovirus latent infection on myeloid progenitor cell gene expression. *J Virol* 2004; 78(8): 4054-4062.
 15. Nam JH, Hwang KA, Yu C H, et al. Expression of interferon inducible genes following Hantaan virus infection as a mechanism of resistance in A549 cells. *Virus Genes* 2003; 26(1): 31-38.
 16. Defilippis V, Raggo C, Moses A, et al. Functional genomics in virology and antiviral drug discovery. *Trends Biotechnol* 2003; 21(10): 452-457.
 17. Leong W F, Tan H C, Ooi E E, et al. Microarray and real-time RT-PCR analyses of differential human gene expression patterns induced by severe acute respiratory syndrome (SARS) coronavirus infection of Vero cells. *Microbes Infect* 2005; 7(2): 248-259.
 18. Zhu H, Cong JP, Mamtora G, et al. Cellular gene expression altered by human cytomegalovirus: global monitoring with oligonucleotide arrays. *Proc Natl Acad Sci U S A* 1998; 95(24): 14470-14475.
 19. Zhu H, Cong JP, Shenk T. Use of differential display analysis to assess the effect of human cytomegalovirus infection on the accumulation of cellular RNAs: induction of interferon-responsive RNAs. *Proc Natl Acad Sci USA* 1997; 94(25): 13985-13990.
 20. Takahashi K, Sawasaki Y, Hata J, et al. Spontaneous transformation and immortalization of human endothelial cells. *In Vitro Cell Dev Biol* 1990; 26(3 Pt 1): 265-274.
 21. Casarosa P, Gruijthuisen YK, Michel D, et al. Constitutive signaling of the human cytomegalovirus-encoded receptor UL33 differs from that of its rat cytomegalovirus homolog R33 by promiscuous activation of G proteins of the Gq, Gi, and Gs classes. *J Biol Chem* 2003; 278(50): 50010-50023.
 22. Vischer HF, Leurs R, Smit MJ. HCMV-encoded G-protein-coupled receptors as constitutively active modulators of cellular signaling networks. *Trends Pharmacol Sci* 2006; 27(1): 56-63.
 23. Vasa-Nicotera M, Brouillette S, Mangino M, et al. Mapping of a major locus that determines telomere length in humans. *Am J Hum Genet* 2005; 76(1): 147-151.
 24. Colberg-Poley A M, Santomena LD. Selective induction of chromosomal gene expression by human cytomegalovirus. *Virology*, 1988; 166(1): 217-228.
 25. Wade M, Kowalik TF, Mudryj M, et al. E2F mediates dihydrofolate reductase promoter activation and multiprotein complex formation in human cytomegalovirus infection. *Mol Cell Biol* 1992; 12(10): 4364-4374.
 26. Jault FM, Jault JM, Ruchti F, et al. Cytomegalovirus infection induces high levels of cyclins, phosphorylated Rb, and p53, leading to cell cycle arrest. *J Virol*, 1995; 69(11): 6697-6704.
 27. Albrecht T, Boldogh I, Fons M, et al. Cell-activation responses to cytomegalovirus infection relationship to the phasing of CMV replication and to the induction of cellular damage. *Subcell Biochem* 1989; 15: 157-202.
 28. Nadeau V, Guillemette S, Belanger L F, et al. Map2k1 and Map2k2 genes contribute to the normal development of syncytiotrophoblasts during placentation. *Development* 2009; 136(8): 1363-1374.
 29. Donaldson P T, Alexander G J, O'Grady J, et al. Evidence for an immune response to HLA class I antigens in the vanishing-bileduct syndrome after liver transplantation. *Lancet* 1987; 1(8539): 945-951.
 30. Vierling J M, Fennell R J. Histopathology of early and late human hepatic allograft rejection: evidence of progressive destruction of interlobular bile ducts. *Hepatology* 1985; 5(6): 1076-1082.